



# An in situ and real-time analytical method for detection of freeze-thaw cycles in tuna via IKnife rapid evaporative ionization mass spectrometry

Zhifeng Shen<sup>a</sup>, Honghai Wang<sup>a</sup>, Jingjing Liang<sup>b,d</sup>, Qiaoling Zhao<sup>c</sup>, Weibo Lu<sup>a</sup>, Yiwei Cui<sup>a</sup>,  
Pinyang Wang<sup>c</sup>, Qing Shen<sup>a,\*</sup>, Jian Chen<sup>a,\*</sup>

<sup>a</sup> Collaborative Innovation Center of Seafood Deep Processing, Zhejiang Province Joint Key Laboratory of Aquatic Products Processing, Institute of Seafood, Zhejiang Gongshang University, Hangzhou, China

<sup>b</sup> Zhejiang Provincial Institute for Food and Drug Control, Hangzhou 310052, China

<sup>c</sup> Zhoushan Institute of Food & Drug Control, Zhoushan 316000, China

<sup>d</sup> Key Laboratory of Quality and Safety of Functional Food for State Market Regulation

## ARTICLE INFO

### Keywords:

Freeze-thaw cycle  
Bluefin tuna  
Lipidomics  
Fatty acids  
Rapid evaporative ionization mass spectrometry (REIMS)

## ABSTRACT

Freezing is one of the most commonly used preservation methods for Bluefin tuna (*Thunnus orientalis*). However, repeated freezing and thawing would inevitably occur due to the temperature fluctuation, leading to the microstructure damage, lipid oxidation and protein integrity decline of tuna muscle without notable visual appearance change. In this study, we used a rapid evaporative ionization mass spectrometry (REIMS) technique for the real-time determination of the extent of repeated freezing and thawing cycles in tuna fillets. We found significant variance in the relative abundance of fatty acids between bluefin tuna and its fresh counterpart following freeze-thaw cycles. Meanwhile, the difference is statistically significant ( $p < 0.05$ ). The quality of tuna remains largely unaffected by a single freeze-thaw cycle but significantly deteriorates after freeze-thaw cycles (freeze-thaw count  $\geq 2$ ), and the relative fatty acid content of the ionized aerosol analysis in the REIMS system positively correlated with the number of freeze-thaw cycles. Notably, palmitic acid (C 16:0,  $m/z$  255.23), oleic acid (C 18:1,  $m/z$  281.24), and docosahexaenoic acid (C 22:6,  $m/z$  327.23) displayed the most pronounced changes within the spectrum of fatty acid groups.

## 1. Introduction

Bluefin tuna (*Thunnus orientalis*) is a popular seafood consumed worldwide due to its high nutritional value and delicious flavor. It is also a significant source of polyunsaturated fatty acids (PUFAs) known for their health benefits (Lee et al., 2022; Lehel et al., 2021; Messina et al., 2022). Specifically, eicosapentaenoic acid (EPA) and docosahexaenoic acid (DHA) in bluefin tuna are linked to various health advantages such as promoting brain development, reducing nerve damage, offering anti-inflammatory properties, and regulating blood pressure and lipid levels (Singh, 2020). Fatty acids are a key component of tuna and may be influenced by changes in external conditions (Sardenne et al., 2017). Therefore, the fatty acid profile could be a good indicator of any changes in the quality of tuna (Domingues et al., 2021).

Temperature fluctuations can have a significant impact on the quality of tuna products (Moriya et al., 2021). In particular, the freeze-thaw cycle can be detrimental to food quality (Hassoun et al., 2020).

Despite the advanced cold chain logistics system in place to maintain temperature stability during transportation, it is inevitable that some fish products will experience temperature variations during shipping, packaging, warehousing, and other processes along the supply chain (Lv & Xie, 2021). Additionally, the mislabeling of thawed fish as fresh is a widespread issue globally (Sotelo et al., 2018). It is essential for consumers to be informed if a product has defrosted, as thawed fish poses a potential risk due to rapid deterioration. Therefore, there is a pressing need for a quick method to determine whether a product has undergone freeze-thaw cycles and to assess its final quality.

Research shows that freeze-thaw cycles can significantly alter the quality of food. These cycles reduce the fat, protein, and lactose content while increasing the dispersion index of the product (Yu et al., 2021). Freeze-thawing can also lead to an increase in free water content and muscle fiber gaps, causing mechanical damage to the original structure (Hallier et al., 2008). Various methods are currently used to identify freeze-thaw cycles and analyze food properties. Gas chromatography

\* Corresponding authors.

E-mail addresses: [leonqshen@163.com](mailto:leonqshen@163.com) (Q. Shen), [chenjian@mail.zjgsu.edu.cn](mailto:chenjian@mail.zjgsu.edu.cn) (J. Chen).

<https://doi.org/10.1016/j.fochx.2024.101705>

Received 2 April 2024; Received in revised form 22 June 2024; Accepted 25 July 2024

Available online 5 August 2024

2590-1575/© 2024 The Authors. Published by Elsevier Ltd. This is an open access article under the CC BY-NC-ND license (<http://creativecommons.org/licenses/by-nc-nd/4.0/>).

(GC) and hydrophilic interaction chromatography with mass spectrometry (HILIC-MS) are commonly used to determine the composition of fatty acids (Moneeb et al., 2021; Yu et al., 2019). Spectral imaging technology with component analysis is also applied to identify fresh and freeze-thawed products (Hassoun et al., 2020; Marlard et al., 2019). Additionally, histology, electrophoresis, and LC-MS have applications in the identification of freeze-thaw products (Ethuin et al., 2015; Stella et al., 2022; Tinacci et al., 2018). These methods have drawbacks such as requiring sample pretreatment, taking a long time, or being unable to produce analysis results in real-time. There is a need to establish a real-time and rapid detection method based on lipidomics analysis of fatty acids.

Recently, rapid evaporation ionization mass spectrometry (REIMS) has emerged as a fast detection technology based on lipidomics (De Graeve et al., 2023; Jones et al., 2019). This technology combines rapid evaporation ionization and an electric surgical scalpel to enable real-time analysis of samples without preprocessing. It identifies samples based on the composition of target compounds within them (Lu et al., 2022; Shen et al., 2020). When tissue cutting is performed using an intelligent surgical knife, aerosols are released and directed into the mass spectrometry detection system through a Venturi pump. This process generates a REIMS mass spectral fingerprint, and the resulting data files allow complex chemometric models to be generated, against which unknown samples can be assessed for their class attributes. Preliminary research has found that the classification accuracy of this technology for identifying tuna adulteration exceeds 90% (Song, Chen, et al., 2020). REIMS has found applications in various fields, including product identification (Rigano et al., 2019; Song et al., 2019), detecting product adulteration, and traceability (Black et al., 2017; Cui et al., 2021, 2022).

This study established a rapid method for identifying whether bluefin tuna has undergone freeze-thaw cycles using rapid evaporation ionization mass spectrometry and lipidomics. The research results will facilitate the quick assessment of fish meat quality, providing valuable insights for product identification and cold chain monitoring.

## 2. Materials and methods

### 2.1. Materials and reagents

Bluefin tuna (*Thunnus orientalis*), sourced from the Hangzhou Huancheng North Road store (Zhejiang Dayang Family Co., Ltd., China). After catching the bluefin tuna in the Pacific fishing grounds, the company's fleet treated it with ultra-low temperature fish body treatment. Each step was maintained under ultra-low temperature conditions of  $-60^{\circ}\text{C}$ . Ultrapure deionized water ( $18.2\text{ M}\Omega\text{-cm}$ ) was produced using a Milli-Q system (Millipore, Bedford, USA). Chromatographic-grade propylene glycol, acquired from Sigma-Aldrich in the USA, was used as the organic solvent. Leucine enkephalin (purity 97%) was procured from Sigma-Aldrich (St. Louis, MO, USA). Phosphate buffer solution (PBS, pH 7.2–7.4) was acquired from Biosharp (USA).

### 2.2. REIMS analysis

The bluefin tuna was cut into fillets measuring  $50\text{ mm} \times 30\text{ mm} \times 5\text{ mm}$  and then divided randomly into four groups: Fresh tuna group (FT), single freeze-thaw tuna group (SFT), twice freeze-thaw tuna group (TFT), and multiple freeze-thaw tuna group (MFT). The fillets were frozen at  $-80^{\circ}\text{C}$  for one day and then thawed with running water to reach room temperature. To ensure the signal strength of the equipment, the fish fillets were moistened with pure water to produce enough aerosols. No further processing was required for the fish fillets, which were cut using the monopolar electrosurgical handpiece (Merun, Wuhan, China) in conjunction with the REIMS system (Waters, UK). Real-time online mass spectrometry analysis was performed on the aerosols generated during the cutting of the fish fillets. The REIMS

analysis was conducted by using the Xevo G2-XS Q-TOF MS quadrupole time-of-flight mass spectrometer (Waters, UK). The monopole electric knife head featured a  $4\text{ m} \times 4.11\text{ mm}$  outer diameter and a  $2.53\text{ mm}$  inner diameter polytetrafluoroethylene tube (PTFE) at the atmospheric interface of the mass spectrometer. As the electric knife cut the fillet, the aerosol produced during the cutting process was conveyed through the PTFE tube using a Venturi pump into the REIMS source. Upon reaching the REIMS interface, the aerosol mixed with isopropanol, which flowed at  $100\text{ }\mu\text{L}/\text{min}$  and contained  $0.2\text{ mg}/\text{mL}$  of leucine enkephalin. Before conducting the test, the detection system was calibrated with leucine enkephalin, which served as an external mass-locking compound with a phase-locking mass charge ratio of  $m/z\ 554.26$ . In the negative ion mode, the selected mass spectrum scanning range was  $m/z\ 50\text{--}1200$ , with a scanning time of  $0.5\text{ s}$ , and the cutting voltage of the electronic scalpel was set to  $20\text{ V}$ . Under these conditions, the total ion current (TIC) signal of the sample was strong. Performing eight repeated cuts for each sample resulted in numerous spectral repetitions and effective peaks, facilitating the creation of a reliable multivariate statistical analysis model.

### 2.3. Free fatty acid (FFA) analysis

The sample was homogenized in PBS (1:10 m/v). Enzyme-linked immunosorbent (ELISA, Coaibo Bio. Co., LTD, Shanghai, China) was used to detect free fatty acid in bluefin tuna. The kit was stabilized at room temperature for 1 h, following the instructions for testing. Absorbance was measured at  $450\text{ nm}$  using SpectraMax 190 absorbance microplate reader (Meigu Molecular Instruments Co., LTD, Shanghai).

### 2.4. Statistical analysis

For data acquisition, MassLynx 4.1 software (Waters, UK) was utilized with spectral noise reduction, selecting peaks with a signal-to-noise (S/N) value exceeding 10 as target peaks. The mass spectrum data, focusing on the fatty acid range of  $m/z\ 200\text{--}400$ , was screened and organized using Microsoft Excel 2019. The LIPIDMAPS prediction tool was employed to identify the fatty acid composition. Mathematical fitting models, including principal component analysis (PCA), were established using multivariate statistical analysis methods. Multivariate statistical analysis charts, such as PCA, partial least squares discriminant analysis (PLS-DA), and heatmap were generated using the online platform (<https://www.chiplot.online/>). Significance analysis was performed using IBM SPSS Statistics 24, with a significance level set at  $p < 0.05$ .

## 3. Results and discussion

### 3.1. Mass spectrometry identification

We measured the total ion current chromatogram (TIC) resulting from three consecutive cuts on the tissue surface of bluefin tuna in the negative ion mode (Fig. 1 (A)). These three consecutive peaks are sourced from the same sample for ensuring biological reproducibility. By performing three repeats, we aimed to enhance the validity of our multivariate statistical analysis model through a sufficient number of spectral repetitions. Fig. 1 (B) displays the mass spectrum data within the  $m/z$  range of  $50\text{--}1200$ , showing that the main characteristic peaks in the negative ion mode are related to fatty acids and phospholipids, with the fatty acid peaks being more prominent. Moreover, Fig. 1 (C) provides insight into the molecular composition of fatty acids within the mass/charge ratio of  $m/z\ 200\text{--}400$ , highlighting significant mass/charge ratios at  $m/z\ 255.24$ ,  $m/z\ 281.25$ ,  $m/z\ 301.22$ , and  $m/z\ 327.23$ .

Mass spectrometry can produce complex mass spectra with overlapping ion peaks, making it challenging to identify and quantify compounds. However, rapid evaporation ionization mass spectrometry enables quick acquisition of response values of fatty acid molecules after

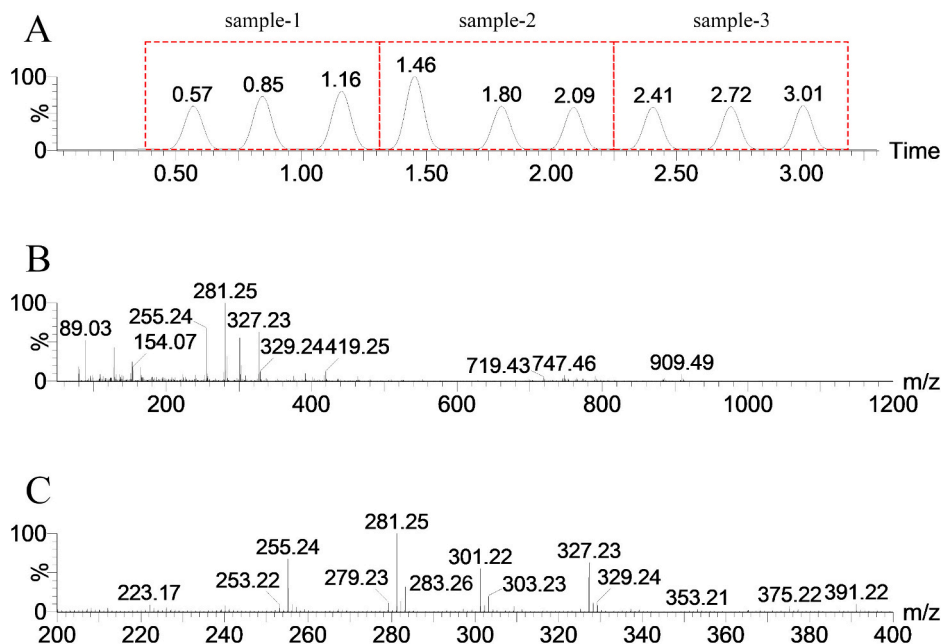


**Fig. 1.** (A) Time-dependent REIMS spectrum of total ion current chromatogram (TIC), obtained with three consecutive cuts of three bluefin tuna fillets; (B) Mass spectra of bluefin tuna lipids in the mass-to-charge ratio range of  $m/z$  50–1200; (C) Fatty acid (FA) mass spectra of bluefin tuna in the mass-to-charge ratio range of  $m/z$  200–400.

data normalization. Fig. 1(C) provides a clear representation of the mass charge data for primary fatty acid components in bluefin tuna. In REIMS, fatty acids ionize by deprotonation, forming  $[M-H]^-$  ion groups. For further analysis, peaks with a signal-to-noise (S/N) value  $>10$  were selected as target peaks (Cui et al., 2022). As shown in Fig. 1, within this range, 13 significant peaks with mass-to-charge ratios between  $m/z$  200–400 are evident, including  $m/z$  223.17,  $m/z$  253.21,  $m/z$  255.23,  $m/z$  279.23,  $m/z$  281.24,  $m/z$  283.26,  $m/z$  301.21,  $m/z$  303.23,  $m/z$  309.27,  $m/z$  327.23,  $m/z$  329.24,  $m/z$  375.32, and  $m/z$  391.35. The molecules were identified using the LIPIDMAPS prediction tool and existing studies (<https://www.lipidmaps.org/>). Predictive tools suggest that these thirteen peaks are ion peaks of fatty acids.

The relative abundance of fatty acids detected using different treatment methods varied, as indicated by previous studies (Shen et al., 2022; Song, Li, et al., 2020). This suggests that analyzing fatty acid abundance can help determine whether the tuna has undergone the freeze-thaw cycle. According to the relative abundance attribution in Table 1, the fatty acid composition of bluefin tuna includes palmitic acid (C 16:0,  $m/z$  255.23), oleic acid (C 18:1,  $m/z$  281.24), stearic acid (C 18:0,  $m/z$  283.26), EPA (C 20:5,  $m/z$  301.21), arachidonic acid (C 20:4,  $m/z$  303.23), and DHA (C 22:6,  $m/z$  327.23). Among these fatty acids, palmitic acid (C 16:0,  $m/z$  255.23), oleic acid (C 18:1,  $m/z$  281.24), and DHA (C 22:6,  $m/z$  327.23) are more abundant. In the fresh tuna group (FT), they accounted for 20.30%, 23.35%, and 15.03% of total fatty acids, respectively. In the single freeze-thaw tuna group (SFT), these figures were 19.61%, 22.70%, and 16.45%, and in the twice freeze-thaw tuna group (TFT), they were 18.37%, 23.05%, and 16.88%. Lastly, the multiple freeze-thaw tuna group (MFT) exhibited contents of 17.47%, 23.56%, and 17.99%, respectively. However, as the number of freeze-thaw cycles increases, the relative standard deviation between groups increases, as shown in Table 1.

303.23), and DHA (C 22:6,  $m/z$  327.23). Among these fatty acids, palmitic acid (C 16:0,  $m/z$  255.23), oleic acid (C 18:1,  $m/z$  281.24), and DHA (C 22:6,  $m/z$  327.23) are more abundant. In the fresh tuna group (FT), they accounted for 20.30%, 23.35%, and 15.03% of total fatty acids, respectively. In the single freeze-thaw tuna group (SFT), these figures were 19.61%, 22.70%, and 16.45%, and in the twice freeze-thaw tuna group (TFT), they were 18.37%, 23.05%, and 16.88%. Lastly, the multiple freeze-thaw tuna group (MFT) exhibited contents of 17.47%, 23.56%, and 17.99%, respectively. However, as the number of freeze-thaw cycles increases, the relative standard deviation between groups increases, as shown in Table 1.

### 3.2. Multivariate statistical analysis

Principal component analysis (PCA) is a statistical method used to reduce the dimensionality of multidimensional data to a few variables. It aims to maintain as much of the original information as possible and visualize the dispersion and distribution of the analyzed data through a score chart (Esteki et al., 2020). Recently, studies have combined PCA and REIMS techniques to investigate the biological origin, geographical

**Table 1**

Relative abundance and attribution of groups in the fatty acid mass charge ratio range of  $m/z$  200–400 in freeze-thaw samples.

$m/z$	Fatty acids	Probable attribution	Abundance (%)			
			FT	STF	TFT	MFT
223.17	Tetradecadienoic acid	[M-H]- FA 14:2	0.44 ± 0.01 <sup>a</sup>	0.44 ± 0.02 <sup>a</sup>	0.19 ± 0.19 <sup>b</sup>	0.06 ± 0.13 <sup>b</sup>
253.21	Palmitoleic acid	[M-H]- FA 16:1	0.32 ± 0.15 <sup>a</sup>	0.47 ± 0.13 <sup>b</sup>	0.81 ± 0.06 <sup>c</sup>	0.94 ± 0.09 <sup>c</sup>
255.23	Palmitic acid	[M-H]- FA 16:0	4.05 ± 0.61 <sup>a</sup>	5.00 ± 1.34 <sup>a</sup>	8.46 ± 0.78 <sup>b</sup>	9.50 ± 0.78 <sup>b</sup>
279.23	Linoleic acid	[M-H]- FA 18:2	0.62 ± 0.09 <sup>a</sup>	0.65 ± 0.32 <sup>a</sup>	1.22 ± 0.13 <sup>b</sup>	1.47 ± 0.18 <sup>b</sup>
281.24	Oleic acid	[M-H]- FA 18:1	4.66 ± 0.69 <sup>a</sup>	5.79 ± 1.41 <sup>a</sup>	10.62 ± 1.45 <sup>b</sup>	12.81 ± 1.02 <sup>c</sup>
283.26	Stearic acid	[M-H]- FA 18:0	1.97 ± 0.46 <sup>a</sup>	2.17 ± 0.48 <sup>a</sup>	3.77 ± 0.30 <sup>b</sup>	4.82 ± 0.65 <sup>c</sup>
301.21	Eicosapentaenoic acid	[M-H]- FA 20:5	2.12 ± 0.45 <sup>a</sup>	2.82 ± 1.35 <sup>a</sup>	6.57 ± 0.72 <sup>b</sup>	7.39 ± 1.04 <sup>b</sup>
303.23	Arachidonic acid	[M-H]- FA 20:4	1.00 ± 0.17 <sup>a</sup>	1.37 ± 0.42 <sup>a</sup>	2.70 ± 0.37 <sup>b</sup>	3.17 ± 0.36 <sup>b</sup>
309.27	Gondoic acid	[M-H]- FA 20:1	0.00 ± 0.00 <sup>a</sup>	0.33 ± 0.13 <sup>b</sup>	0.62 ± 0.10 <sup>c</sup>	0.68 ± 0.08 <sup>c</sup>
327.23	Docosahexaenoic acid	[M-H]- FA 22:6	3.00 ± 0.51 <sup>a</sup>	4.20 ± 1.48 <sup>a</sup>	7.77 ± 1.26 <sup>b</sup>	9.79 ± 1.04 <sup>c</sup>
329.24	Docosapentaenoic acid	[M-H]- FA 22:5	0.50 ± 0.08 <sup>a</sup>	0.70 ± 0.25 <sup>a</sup>	1.35 ± 0.16 <sup>b</sup>	1.65 ± 0.23 <sup>c</sup>
375.32	Eicosapentaenoic acid	[M-H]- FA 25:3	0.55 ± 0.08 <sup>a</sup>	0.66 ± 0.10 <sup>ab</sup>	0.79 ± 0.19 <sup>bc</sup>	0.95 ± 0.14 <sup>c</sup>
391.35	Hexacosadienoic acid	[M-H]- FA 26:2	0.73 ± 0.10 <sup>a</sup>	0.91 ± 0.18 <sup>b</sup>	1.19 ± 0.11 <sup>c</sup>	1.16 ± 0.10 <sup>c</sup>

Different letters represent significant differences.

origin, and composition authenticity of tuna (Song, Chen, et al., 2020). In order to determine the difference in fatty acid composition between fresh and freeze-thawed bluefin tuna samples, a multivariate statistical analysis was conducted. PCA was chosen as the method for dimensionality reduction, which minimized data loss while reducing the

dimensionality of the collected multivariate scattered information. Fig. 2(A) showed that both the twice freeze-thaw tuna group (TFT) and multiple freeze-thaw tuna group (MFT) were significant segregated from the fresh tuna group (FT). The single freeze-thaw tuna group (SFT) and twice freeze-thaw tuna group (TFT) treatment groups were significantly

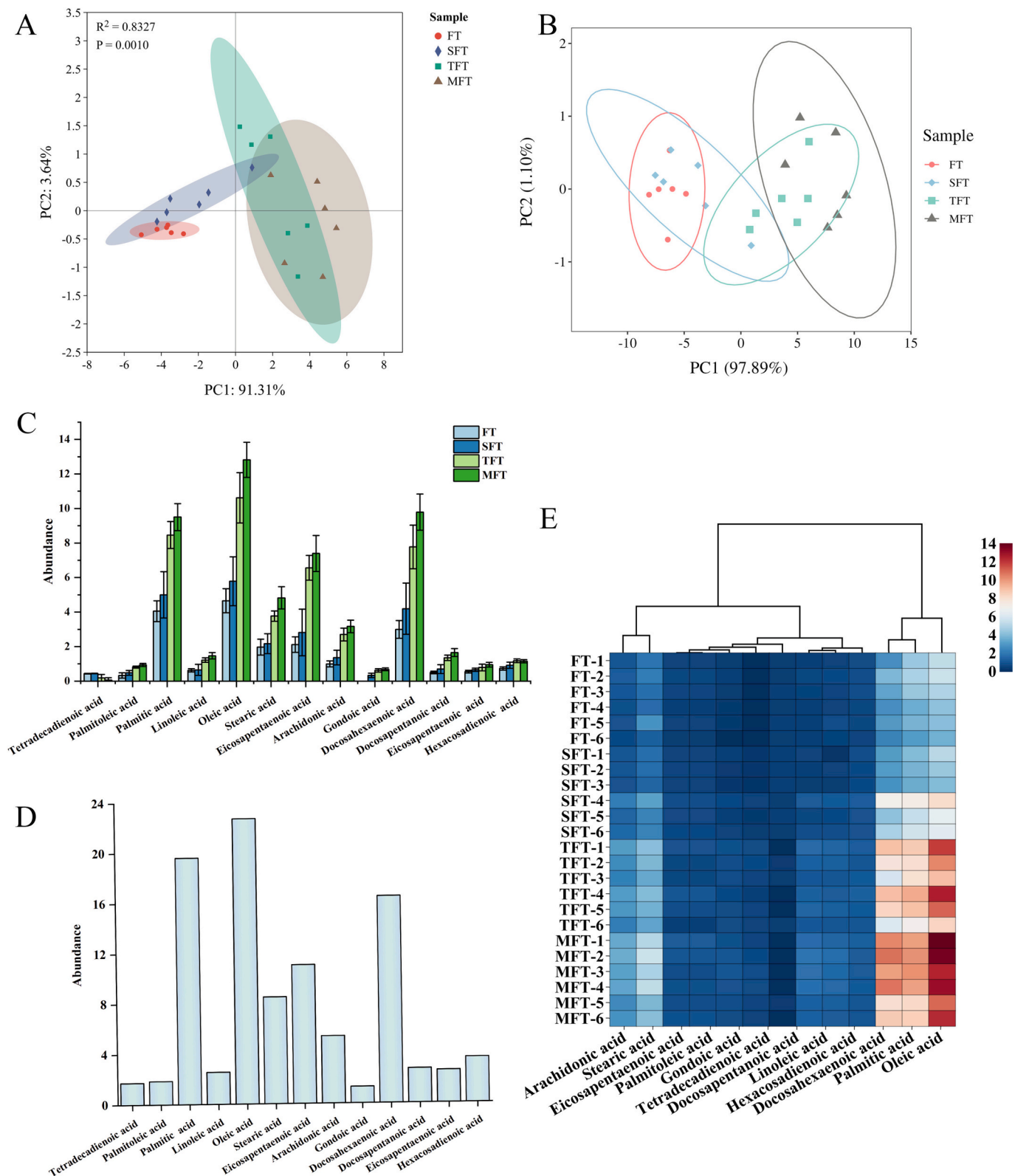


Fig. 2. (A) Principal component analysis diagram; (B) PLS-DA score chart; (C) Schematic diagram of the molecular relative abundance of fatty acids; (D) VIP score chart; (E) Heat map of the fatty acid cluster.

segregated and clustered insignificantly. This suggests that freezing and thawing may cause changes in the material inside. It indicates that a single freeze-thaw cycle has a negligible impact on the fatty acid composition of bluefin tuna, whereas repeated freeze-thaw cycles significantly alter it. PCA analysis results highlight the observable changes in tuna fatty acid composition after undergoing a freeze-thaw cycle, with limited influence after a single freeze-thaw event.

PLS-DA is a partial least squares regression model, effectively distinguishing values between groups. Unlike PCA, which is unsupervised and finds trends in the data without using class information, PLS-DA is supervised and aims to separate the classes as much as possible in a multi-dimensional space. It overcomes the limitations of PCA by differentiating all samples and successfully addresses the drawbacks of unsupervised analysis. In Fig. 2(B), it is evident that there is minimal distinction between the fresh tuna group (FT) group and the single freeze-thaw tuna group (SFT), with some overlap of samples within each group. The twice freeze-thaw tuna group (TFT) presents a broad sample distribution, although some individuals closely resemble the control group. In contrast, the multiple freeze-thaw tuna group (MFT) group samples are completely segregated from the control group, indicating a significant difference. Fig. 2(B) shows that bluefin tuna undergoes gradual changes in fatty acids throughout the freeze-thaw cycle. A single freeze-thaw event has a marginal effect on fatty acids, with differences becoming more pronounced as freeze-thaw frequency increases.

The charts provided in Fig. 2(C) and Fig. 2(D) illustrate changes in the abundance of fatty acids in bluefin tuna as a result of the freeze-thaw process. Specifically, 13 fatty acid ions, including palmitic acid (C 16:0,  $m/z$  255.23), oleic acid (C 18:1,  $m/z$  281.24), stearic acid (C 18:0,  $m/z$  283.26), EPA (C 20:5,  $m/z$  301.21), arachidonic acid (C 20:4,  $m/z$  303.23), and DHA (C 22:6,  $m/z$  327.23), exhibited significant changes. The relative abundance of these fatty acids is shown to increase with the frequency of freeze-thaw cycles, suggesting that bluefin tuna lipids break down into different fatty acid molecules during the freeze-thaw process, consequently impacting fish quality.

To visually compare the shifts in fatty acid relative abundance in tuna subjected to repeated freezing and thawing, a cluster heat map analysis was performed (Fig. 2(E)). The fatty acid cluster heat map intuitively represents the relative abundance data using color, with color intensity indicating data values. This heat map intuitively represents the relative abundance data using color, with darker and redder colors indicating higher relative substance abundance. It provides insights into the similarities and differences in fatty acid abundance within and between sample groups. It illustrates the similarities and differences in fatty acid abundance within and between sample groups. Each quadrilateral, after normalization of sample fatty acid distribution, represents the relative abundance of an ion, visualized by color characterization. The results show varying degrees of increase in fatty acid content in bluefin tuna after repeated freeze-thaw cycles, likely associated with lipid decomposition reactions.

### 3.3. Method validation

Based on the accuracy of the REIMS method for real-time identification of bluefin tuna undergoing freeze-thaw cycles, as indicated by the inter-day and intra-day precision expressed using relative standard deviation (RSD) (Lu et al., 2022), the result summarized in Table 2. Using

**Table 2**  
Relative standard deviation between intra-day and inter-day.

Sample	Relative standard deviation (RSD)	
	Intra-day	Inter-day
FT	5.02%	9.88%
SFT	6.93%	15.85%
TFT	5.17%	14.41%
MFT	1.73%	9.36%

fresh samples as a reference, fatty acid ions (such as palmitic acid, oleic acid) with high relative abundance were selected as representative ions. Intra-day precision was calculated by the error of three repeated ionizations of the tuna sample in the same batch, while inter-day precision involved the analysis of the sample for three consecutive days. The results in Table 2 show that the intra-day precision of the target ions is <7%, and the inter-day precision of the target ions ranges between 9% and 16%. Our findings indicate that the method demonstrates good repeatability during the intra-day and can provide reference during the inter-day. The difference in inter-day precision in the SFT group may be related to the decomposition of fatty acids after freezing and thawing. In the PCA analysis (Fig. 2(A)), the single freeze-thaw tuna group (SFT) overlaps with both the fresh tuna group (FT) and the twice freeze-thaw tuna group (TFT), indicating a transition from the fresh tuna group (FT) to the twice freeze-thaw tuna group (TFT). Therefore, we believe that the difference in daytime precision may be related to the change of fatty acids after freezing and thawing, leading to an increased difference. (See Table 3.)

The freeze-thaw treatment increases the content of free fatty acids in fish samples, mainly due to the breakdown of some phospholipids and neutral lipids by lipase. Fish with a high fat content are more susceptible to damage. The standard curve, drawn by the absorbance of the FFA standard at 450 nm, is shown in Fig. 3(A). The content of free fatty acids in bluefin tuna undergoing freeze-thaw cycles is depicted in Fig. 3(B). After freeze-thaw cycles, the content of free fatty acids increased significantly, especially after two freeze-thaw cycles. This result is consistent with that of multivariate statistical analysis, which verifies the feasibility of the REIMS method. We suspected that the increase in free fatty acids is due to the breakdown of lipids during the freeze-thaw cycle.

## 4. Conclusions

The iKnife-REIMS method, based on lipidomics, has been shown to be effective in determining whether bluefin tuna has undergone freeze-thaw cycles. In the negative ion mode, there are significant differences in fatty acid relative abundance between fresh bluefin tuna samples and those that have been through freeze-thaw cycles. However, there is no significant difference between fresh bluefin tuna and samples that have undergone a single freeze-thaw cycle. This suggests that the quality of tuna remains largely unaffected by a single freeze-thaw cycle during transportation but deteriorates significantly after multiple cycles (freeze-thaw count  $\geq 2$ ). Through multivariate statistical analysis, we identified various fatty acid ions, including palmitic acid (C 16:0,  $m/z$  255.23), oleic acid (C 18:1,  $m/z$  281.24), and DHA (C 22:6,  $m/z$  327.23). These ions could be good indicators of any changes in the quality of tuna. The REIMS method appears to be a useful tool for quickly identifying bluefin tuna that has been subjected to freeze-thaw cycles, aiding in food adulteration detection and screening for cold chain faults. Further research is needed to distinguish differences between single freeze-thaw and fresh samples.

## Ethical approval

This article does not contain studies with human participants. All

**Table 3**  
chemical compounds studied in the article.

NO.	Name	Molecular Formula	CAS NO.
1	Isopropyl Alcohol	C <sub>3</sub> H <sub>8</sub> O	67-63-0
2	Leucine enkephalin	C <sub>28</sub> H <sub>37</sub> N <sub>5</sub> O <sub>7</sub>	58,822-25-6
3	Palmitic Acid	C <sub>16</sub> H <sub>32</sub> O <sub>2</sub>	57-10-3
4	Oleic Acid	C <sub>18</sub> H <sub>34</sub> O <sub>2</sub>	112-80-1
5	Stearic Acid	C <sub>18</sub> H <sub>36</sub> O <sub>2</sub>	57-11-4
6	Eicosapentaenoic acid	C <sub>20</sub> H <sub>30</sub> O <sub>2</sub>	10,417-94-4
7	Docosahexaenoic acid	C <sub>22</sub> H <sub>32</sub> O <sub>2</sub>	6217-54-5

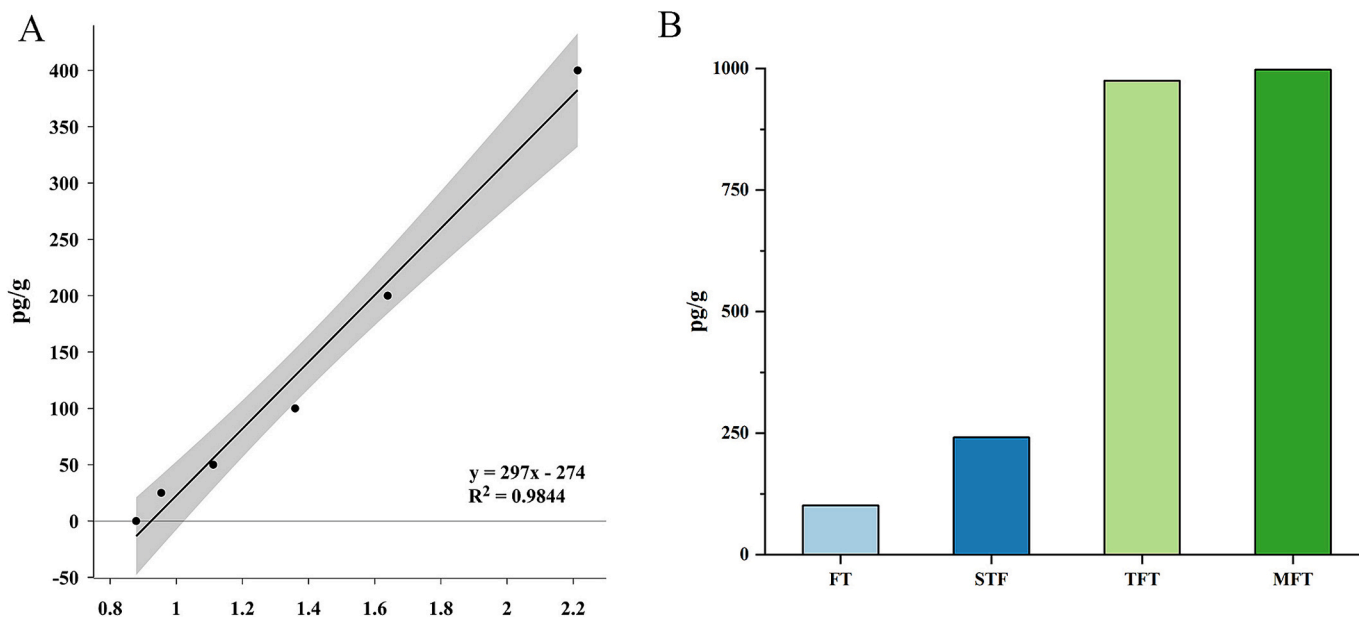


Fig. 3. (A) FFA standard curve; (B) Fatty acid content (pg/g).

applicable international, national, and/or institutional guidelines for the care and use of animals were followed.

#### CRediT authorship contribution statement

**Zhifeng Shen:** Writing – original draft, Methodology. **Honghai Wang:** Methodology. **Jingjing Liang:** Formal analysis. **Qiaoling Zhao:** Methodology. **Weibo Lu:** Data curation. **Yiwei Cui:** Methodology. **Pingya Wang:** Funding acquisition. **Qing Shen:** Methodology, Conceptualization. **Jian Chen:** Supervision, Resources, Conceptualization.

#### Declaration of competing interest

The authors declare that they have no known competing financial interests or personal relationships that could have appeared to influence the work reported in this paper.

#### Data availability

The data that has been used is confidential.

#### Acknowledgments

This work supported by the National Natural Science Foundation of China (32172304), Zhejiang Provincial Public Welfare Technology Research Project (LTGN23C200007, TGN24C200038), Science and Technology Project of State Administration for Market Regulation (2022MK055) and Project of Zhejiang Provincial Food and Drug Administration (2021016, 2021017).

#### References

- Black, C., Chevallier, O. P., Haughey, S. A., Balog, J., Stead, S., Pringle, S. D., ... Elliott, C. T. (2017). A real time metabolomic profiling approach to detecting fish fraud using rapid evaporative ionisation mass spectrometry. *Metabolomics*, 13(12), 153. <https://doi.org/10.1007/s11306-017-1291-y>
- Cui, Y., Ge, L., Lu, W., Wang, S., Li, Y., Wang, H., Huang, M., Xie, H., Liao, J., Tao, Y., Luo, P., Ding, Y.-Y., & Shen, Q. (2022). Real-time profiling and distinction of lipids from different mammalian milks using rapid evaporative ionization mass spectrometry combined with Chemometric analysis. *Journal of Agricultural and Food Chemistry*, 70(25), 7786–7795. <https://doi.org/10.1021/acs.jafc.2c01447>
- Cui, Y., Wang, H., Zhao, Q., Zhu, X., Wang, P., Xue, J., Chen, K., & Shen, Q. (2021). Real-time detection of authenticity and adulteration of krill phospholipids with soybean phospholipids using rapid evaporative ionization mass spectrometry: Application on commercial samples. *Food Control*, 121, Article 107680. <https://doi.org/10.1016/j.foodcont.2020.107680>
- De Graeve, M., Birse, N., Hong, Y., Elliott, C. T., Hemeryck, L. Y., & Vanhaecke, L. (2023). Multivariate versus machine learning-based classification of rapid evaporative ionisation mass spectrometry spectra towards industry based large-scale fish speciation. *Food Chemistry*, 404, Article 134632. <https://doi.org/10.1016/j.foodchem.2022.134632>
- Domingues, V. F., Quaresma, M., Sousa, S., Rosas, M., Ventoso, B., Nunes, M. L., & Delerue-Matos, C. (2021). Evaluating the lipid quality of yellowfin tuna (*Thunnus albacares*) harvested from different oceans by their fatty acid signatures. *Foods*, 10(11), 2816. <https://doi.org/10.3390/foods10112816>
- Esteki, M., Shahsavari, Z., & Simal-Gandara, J. (2020). Gas chromatographic fingerprinting coupled to Chemometrics for food authentication. *Food Reviews International*, 36(4), 384–427. <https://doi.org/10.1080/87559129.2019.1649691>
- Ethuin, P., Marlard, S., Delosièrre, M., Carapito, C., Delalande, F., Van Dorsselaer, A., Dehaut, A., Lencel, V., Duflos, G., & Grard, T. (2015). Differentiation between fresh and frozen-thawed sea bass (*Dicentrarchus labrax*) fillets using two-dimensional gel electrophoresis. *Food Chemistry*, 176, 294–301. <https://doi.org/10.1016/j.foodchem.2014.12.065>
- Hallier, A., Chevallier, S., Serot, T., & Prost, C. (2008). Freezing-thawing effects on the colour and texture of European catfish flesh. *International Journal of Food Science & Technology*, 43(7), 1253–1262. <https://doi.org/10.1111/j.1365-2621.2007.01601.x>
- Hassoun, A., Shumilina, E., Di Donato, F., Foschi, M., Simal-Gandara, J., & Biancolillo, A. (2020). Emerging Techniques for Differentiation of Fresh and Frozen-Thawed Seafoods: Highlighting the Potential of Spectroscopic Techniques. *Molecules*, 25(19), 4472. <https://doi.org/10.3390/molecules25194472>
- Jones, E. A., Simon, D., Karancsi, T., Balog, J., Pringle, S. D., & Takats, Z. (2019). Matrix assisted rapid evaporative ionization mass spectrometry. *Analytical Chemistry*, 91(15), 9784–9791. <https://doi.org/10.1021/acs.analchem.9b01441>
- Lee, S.-H., Lee, C.-L., Ko, J., & Hong, J.-H. (2022). The role of food stereotype in hedonic judgment of a delicacy food: A case study of Korean consumers' liking for sliced raw fish (sashimi). *Food Research International*, 162, Article 112028. <https://doi.org/10.1016/j.foodres.2022.112028>
- Lehel, J., Yaucat-Guendi, R., Darnay, L., Palotás, P., & Laczay, P. (2021). Possible food safety hazards of ready-to-eat raw fish containing product (sushi, sashimi). *Critical Reviews in Food Science and Nutrition*, 61(5), 867–888. <https://doi.org/10.1080/10408398.2020.1749024>
- Lu, W., Wang, P., Ge, L., Chen, X., Guo, S., Zhao, Q., Zhu, X., Cui, Y., Zhang, M., Chen, K., Ding, Y.-Y., & Shen, Q. (2022). Real-time authentication of minced shrimp by rapid evaporative ionization mass spectrometry. *Food Chemistry*, 383, Article 132432. <https://doi.org/10.1016/j.foodchem.2022.132432>
- Lv, Y., & Xie, J. (2021). Effects of Freeze–Thaw Cycles on Water Migration, Microstructure and Protein Oxidation in Cuttlefish. *Foods*, 10(11), 2576. <https://doi.org/10.3390/foods10112576>
- Marlard, S., Doyen, P., & Grard, T. (2019). Rapid multiparameters approach to differentiate fresh Skinless Sea bass (*Dicentrarchus labrax*) fillets from frozen-thawed ones. *Journal of Aquatic Food Product Technology*, 28(2), 253–262. <https://doi.org/10.1080/10498850.2019.1572257>
- Messina, C. M., Arena, R., Manuguerra, S., La Barbera, L., Curcuraci, E., Renda, G., & Santulli, A. (2022). Valorization of side stream products from sea cage fattened

- Bluefin tuna (*Thunnus thynnus*): Production and in vitro bioactivity evaluation of enriched  $\omega$ -3 polyunsaturated fatty acids. *Marine Drugs*, 20(5), 309. <https://doi.org/10.3390/md20050309>
- Moneeb, A. H. M., Hammam, A. R. A., Ahmed, A. K. A., Ahmed, M. E., & Alsaleem, K. A. (2021). Effect of fat extraction methods on the fatty acids composition of bovine milk using gas chromatography. *Food Science & Nutrition*, 9(6), 2936–2942. <https://doi.org/10.1002/fsn3.2252>
- Moriya, K., Miyazaki, A., Kodama, H., Sakamoto, M., & Ebitani, K. (2021). Influence of ice storage period before freezing on quality of frozen chub mackerel *Scomber japonicus* fillets and considerations regarding high-quality frozen sashimi products. *Fisheries Science*, 87(6), 905–913. <https://doi.org/10.1007/s12562-021-01552-3>
- Rigano, F., Mangraviti, D., Stead, S., Martin, N., Petit, D., Dugo, P., & Mondello, L. (2019). Rapid evaporative ionization mass spectrometry coupled with an electrosurgical knife for the rapid identification of Mediterranean Sea species. *Analytical and Bioanalytical Chemistry*, 411(25), 6603–6614. <https://doi.org/10.1007/s00216-019-02000-z>
- Sardenne, F., Kraffe, E., Amiel, A., Fouché, E., Debrauwer, L., Ménard, F., & Bodin, N. (2017). Biological and environmental influence on tissue fatty acid compositions in wild tropical tunas. *Comparative Biochemistry and Physiology Part A: Molecular & Integrative Physiology*, 204, 17–27. <https://doi.org/10.1016/j.cbpa.2016.11.007>
- Shen, Q., Li, L., Song, G., Feng, J., Li, S., Wang, Y., Ma, J., & Wang, H. (2020). Development of an intelligent surgical knife rapid evaporative ionization mass spectrometry based method for real-time differentiation of cod from oilfish. *Journal of Food Composition and Analysis*, 86, Article 103355. <https://doi.org/10.1016/j.jfca.2019.103355>
- Shen, Q., Song, G., Zhao, Q., Wang, P., Yang, H., Xue, J., Wang, H., Cui, Y., & Wang, H. (2022). Detection of lipidomics characterization of tuna meat during different wet-aging stages using iKnife rapid evaporative ionization mass spectrometry. *Food Research International*, 156, Article 111307. <https://doi.org/10.1016/j.foodres.2022.111307>
- Singh, J. E. (2020). Dietary sources of Omega-3 fatty acids versus Omega-3 fatty acid supplementation effects on cognition and inflammation. *Current Nutrition Reports*, 9(3), 264–277. <https://doi.org/10.1007/s13668-020-00329-x>
- Song, G., Chen, K., Wang, H., Zhang, M., Yu, X., Wang, J., & Shen, Q. (2020). In situ and real-time authentication of *Thunnus* species by iKnife rapid evaporative ionization mass spectrometry based lipidomics without sample pretreatment. *Food Chemistry*, 318, Article 126504. <https://doi.org/10.1016/j.foodchem.2020.126504>
- Song, G., Li, L., Wang, H., Zhang, M., Yu, X., Wang, J., & Shen, Q. (2020). Electric soldering Iron ionization mass spectrometry based Lipidomics for in situ monitoring fish oil oxidation characteristics during storage. *Journal of Agricultural and Food Chemistry*, 68(7), 2240–2248. <https://doi.org/10.1021/acs.jafc.9b06406>
- Song, G., Zhang, M., Zhang, Y., Wang, H., Li, S., Dai, Z., & Shen, Q. (2019). In situ method for real-time discriminating Salmon and Rainbow trout without sample preparation using iKnife and rapid evaporative ionization mass spectrometry-based Lipidomics. *Journal of Agricultural and Food Chemistry*, 67(16), 4679–4688. <https://doi.org/10.1021/acs.jafc.9b00751>
- Sotelo, C. G., Velasco, A., Perez-Martin, R. I., Kappel, K., Schröder, U., Verrez-Bagnis, V., ... Griffiths, A. (2018). Tuna labels matter in Europe: Mislabelling rates in different tuna products. *PLoS One*, 13(5), Article e0196641. <https://doi.org/10.1371/journal.pone.0196641>
- Stella, R., Mastrorilli, E., Pretto, T., Tata, A., Piro, R., Arcangeli, G., & Biancotto, G. (2022). New strategies for the differentiation of fresh and frozen/thawed fish: Non-targeted metabolomics by LC-HRMS (part B). *Food Control*, 132, Article 108461. <https://doi.org/10.1016/j.foodcont.2021.108461>
- Tinacci, L., Armani, A., Guidi, A., Nucera, D., Shvartzman, D., Miragliotta, V., ... Abramo, F. (2018). Histological discrimination of fresh and frozen/thawed fish meat: European hake (*Merluccius merluccius*) as a possible model for white meat fish species. *Food Control*, 92, 154–161. <https://doi.org/10.1016/j.foodcont.2018.04.056>
- Yu, X., Chen, K., Li, S., Wang, Y., & Shen, Q. (2019). Lipidomics differentiation of soft-shelled turtle strains using hydrophilic interaction liquid chromatography and mass spectrometry. *Journal of Chromatography B*, 1112, 11–15. <https://doi.org/10.1016/j.jchromb.2019.02.025>
- Yu, Z., Qiao, C., Zhang, X., Yan, L., Li, L., & Liu, Y. (2021). Screening of frozen-thawed conditions for keeping nutritive compositions and physicochemical characteristics of goat milk. *Journal of Dairy Science*, 104(4), 4108–4118. <https://doi.org/10.3168/jds.2020-19238>